FEBS Letters 554 (2003) 394–398 FEBS 27814

A microscope-based screening platform for large-scale functional protein analysis in intact cells

Urban Liebel[a,1], Vytaute Starkuviene[a,1], Holger Erfle[a], Jeremy C. Simpson[a], Annemarie Poustka[b], Stefan Wiemann[b], Rainer Pepperkok[a,*]

[a] *Cell Biology and Cell Biophysics Programme, European Molecular Biology Laboratory, Meyerhofstrasse 1, 69117 Heidelberg, Germany*
[b] *Molecular Genome Analysis, German Cancer Research Centre, Im Neuenheimer Feld 280/506, 69120 Heidelberg, Germany*

Received 12 September 2003; accepted 30 September 2003

First published online 22 October 2003

Edited by Felix Wieland

Abstract A modular microscope-based screening platform, with applications in large-scale analysis of protein function in intact cells is described. It includes automated sample preparation, image acquisition, data management and analysis, and the genome-wide automated retrieval of bioinformatic information. The modular nature of the system ensures that it is rapidly adaptable to new biological questions or sets of proteins. Two automated functional assays addressing protein secretion and the integrity of the Golgi complex were developed and tested. This shows the potential of the system in large-scale, cell-based functional proteomic projects.

Key words: Green fluorescent protein; Proteomics; Functional analysis; High-content screening microscopy; Membrane traffic; Golgi complex

1. Introduction

The recent completion of the sequencing of entire genomes from various organisms provides the potential to systematically study each and every gene in turn. One of the challenges now is to develop methods that allow large-scale functional studies of the encoded proteins in their natural environment, the living cell. Strategies have been devised to address a first step in revealing protein function by systematically determining protein localisation using green fluorescent protein (GFP)-tagged cDNA libraries or collections of open reading frames (ORFs) [1–4]. These studies also provide novel tools, the GFP-tagged cDNAs, for follow-up studies addressing protein function by fluorescence microscopy, which itself is a powerful technique for in vivo studies as it gives quantitative access to the spatial distribution and dynamics of membrane-bounded organelles, proteins or biochemical reactions in single cells [5,6].

The problem of performing functional microscope-based assays on a large set of proteins in cells is presently still a challenge. It requires automation and coordination of various steps such as sample preparation, image acquisition and the handling and analysis of large sets of image data. Furthermore, integration of the results with existing knowledge on the proteins under investigation such as it is provided by bioinformatic databases is also important. Some automated screening microscopes have already been described and applied or are commercially available [7,8]. Limitations of commercially available systems are often that they have been designed and optimised for special applications, which restricts the possibilities for adaptation to new assays. Systems with ultra-high throughput capacities are lacking the single cell or subcellular resolution and thus provide only specialised information.

Here we describe a modular microscope-based screening platform and its application to the development of two cell-based assays addressing protein secretion and Golgi integrity. This demonstrates its potential for large-scale functional screening projects.

2. Materials and methods

2.1. Materials

GFP-tagged ORFs were generated and prepared as described earlier [3].

The yellow fluorescent protein (YFP)-tagged SAR1 mutant, SAR1-GTP-YFP plasmid, was constructed by transferring the SAR1 (H79G) mutant, from the pSG5 vector into the C1-YFP Clontech vector via *Eco*R1 and *Bam*H1 restriction sites and standard cloning methods. Recombinant adenoviruses encoding the secretory marker protein ts-O45-G tagged with either cyan fluorescent protein (CFP) or YFP were as described [9]. All cell culture reagents were from Gibco/Invitrogen (Karlsruhe, Germany). LabTek eight- and 96-well plates were from Nalge Nunc (Rochester, NY,USA). Cycloheximide and nocodazole were from Calbiochem (San Diego, CA, USA), FuGENE6 was from Roche (Mannheim, Germany), Cy5-labelled anti-mouse secondary antibodies were from Amersham Biosciences (Freiburg, Germany), mouse monoclonal anti-GM130 antibody was from BD Bioscience (San Diego, CA, USA), the mouse monoclonal anti-ts-O45-G antibody VG was a gift from Kai Simons (MPI-CBG, Dresden, Germany), Hoechst 33342 stain was from Sigma (Munich, Germany).

2.2. Hardware and set-up of the screening system

Liquid handling procedures such as DNA transfection and immunostaining were performed on a Multiprobe IIex robot (Perkin Elmer, Wellesley, MA, USA). A special specimen holder carrying four LabTek eight-well chamber slides was developed for automated bi-directional transport between the liquid handling system and the automated microscope.

The automated microscope is built with standard components of an

*Corresponding author. Fax: (49)-6221-387 306.
E-mail address: pepperko@embl-heidelberg.de (R. Pepperkok).

[1] These authors contributed equally to this work.

Abbreviations: CFP, cyan fluorescent protein; ER, endoplasmic reticulum; GFP, green fluorescent protein; ORF, open reading frame; YFP, yellow fluorescent protein

0014-5793/03/$22.00
doi:10.1016/S0014-5793(03)01197-9

Olympus BX system (Olympus-Europe, Hamburg, Germany) and is mounted in a custom-built, anti-vibration aluminium frame. Images are acquired with a cooled CCD camera (SensiCam 1280×1024 pixels, PCO, Kehlheim, Germany). A motorised *xyz*-stage (ASI Instruments, Eugene, OR, USA) allows positioning with a resolution of 0.1 μm. All movable parts of the system are remote controlled by LabView™ (National Instruments, Munich, Germany) software modules that were developed in our laboratory. The robot and microscope are integrated into a glass cabinet to provide sterile conditions. Pictures of the entire system and more detailed information can be viewed at http://www.embl.de/~liebel.

2.3. Automated transfection and immunostaining

For automated transfection and immunostaining the multiprobe robot system was used for each step described below, except for the plating of cells. Cells were plated at a density of 1200 cells/cm^2 in 96-well plates containing 100 μl culture medium/well. Four μl plasmid DNA at a concentration of 50 ng/μl was added to the transfection master mix consisting of FuGENE6 and OPTIMEM 1, which was prepared so that for each well 10 μl liquid contained 9.7 μl OPTIMEM 1 and 0.3 μl FuGENE6. For cell fixation the culture medium was removed and cells were incubated with 75 μl of 3% paraformaldehyde for 20 min at room temperature. For immunostaining 50 μl of the respective antibody solutions were added per well and incubated for 30 min at room temperature. Nuclei were labelled for 5 min with 75 μl Hoechst solution at a concentration of 0.1 μg/ml. All washing steps after cell fixation or antibody staining were performed three times for 5 min, each with 200 μl of phosphate-buffered saline (PBS)/well.

2.4. Protein transport assay

HeLa cells were transfected with plasmid DNAs encoding CFP- or YFP-tagged proteins and 6 h, thereafter they were overlaid with recombinant adenoviruses encoding the secretory marker protein ts-O45-G tagged with CFP or YFP to complement the colour of the transfected CFP- or YFP-tagged protein. After 45 min incubation the cells were washed with culture medium and ts-O45-G was accumulated in the endoplasmic reticulum (ER) by incubating the cells at 39.5°C for 16 h. Thereafter, cells were shifted to 32°C, 60 min in the presence of 100 μg/ml cycloheximide to release ts-O45-G from the ER. Then, cells were fixed with 3% paraformaldehyde and ts-O45-G on the cell surface was detected by immunostaining with a monoclonal antibody (VG) recognising an extracellular ts-O45-G epitope at the plasma membrane followed by staining with Cy5-labelled secondary anti-mouse antibodies. Cell nuclei were labelled with Hoechst 33342 stain diluted in PBS to a final concentration of 0.1 μg/ml.

2.5. Golgi integrity assay

HeLa cells were fixed in 3% paraformaldehyde and permeabilised with 0.1% Triton X-100 and the Golgi complex was stained with mouse monoclonal anti-GM130 antibody followed by Cy5-conjugated anti-mouse secondary antibodies. Cell nuclei were labelled with Hoechst stain as described above.

3. Results and discussion

The screening platform developed consists of modules covering automated cell transfection and immunostaining, image acquisition, data management and analysis, and collection of bioinformatic information from databases. They were developed with the graphical prototyping software provided by LabView and designed to operate independently of each other. Therefore, implementation of further modules or products from different companies for the development of new assays is easily possible. In this way the optimum hard and software components for assay specific tasks can always be used. This is critical for scientific screening platforms such as the one described here, where different fields of expertise have to be combined.

With the protocols developed for automated cell transfection efficiencies of up to 30% could be obtained, which was however two to three times less compared to those obtained by manual transfection. In contrast, immunostaining performed automatically on the robot system (see Figs. 1 and 3) showed a quality that was comparable to experiments conducted manually (not shown). Optimum expression times for different cDNAs varied between 12 and 48 h and therefore transfection efficiencies of different cDNAs on the same 96-well plate varied by a factor of up to 10. This problem could be overcome by transfecting in parallel those cDNAs which showed similar expression kinetics.

The image acquisition module controls automated image acquisition of multistained samples. Screening of an entire 96-well plate when taking 15 fields of view per well lasts between 45 min and 5 h depending on the number of colours in the sample and exposure times used. Critical for obtaining high-quality image data in such systems is the automated identification of the focal plane for each field of view. Solutions that analyse the field of view either as one entity, or by focusing on the plane containing the brightest object, very often determine a focal plane with either only few of the cells in the field or non-relevant structures with a high intensity being in focus. Therefore, we have developed a robust software autofocus routine that analyses each individual cell in the field separately. The plane which contains the maximum number of objects in the field that fulfil user defined 'in focus' criteria is used as the focal plane. In this way, bright dead cells or junk particles do not disturb focus identification. The procedure is independent of the objective and cell type used and achieves similar results for glass and plastic tissue culture plates. In test runs 92% of the images defined by the autofocus as 'in focus' matched also the judgment by manual inspections. More detailed information about this module can be found at www.embl.de/~liebel.

Currently available screening platforms use databases to handle the acquired data. These have project specific structures, which has the disadvantage that new projects or changes in hardware may require time-consuming restructuring. Furthermore, when the platform includes several screening microscopes used in parallel, each of them can only operate when the database is fully functioning, which therefore becomes a bottleneck for the entire platform. We have overcome these problems by using a distributed server concept for storage, retrieval and analysis of acquired image data from multiple independent systems without the need for a database. Meta-information such as the experiment name or well position is saved within the file name of every individual image acquired. For data retrieval, we developed an intranet search engine operating similar to Google™, where index computers screen the system devices for data. In this way the system is able to handle millions of files on different computers or data storage devices.

Once the screening has identified interesting candidate proteins, it is of vital importance to integrate the results with existing bioinformatic knowledge on these proteins. For this purpose we have developed a module that automatically collects for the entire human genome bioinformatic knowledge and predictions from public webservers on a regular basis (harvester.embl.de). In this way bioinformatic data on the proteins under investigation are up to date and instantly available.

Two screening assays, which address protein secretion or

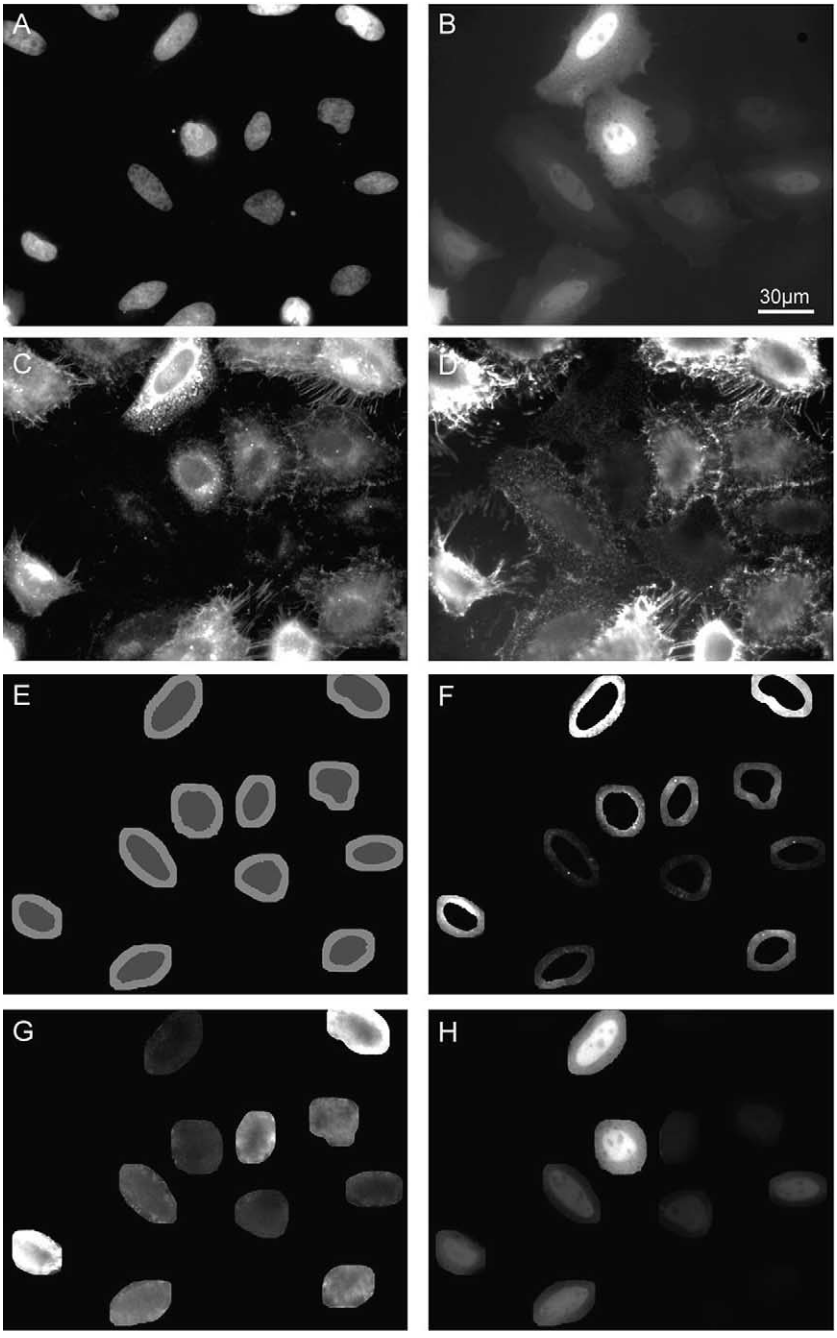

Fig. 1. Example of the automated transport assay and image analysis steps for data analysis. HeLa cells were prepared for the transport assay as described in Section 2. Images of the Hoechst-stained cell nuclei (A), YFP-transfected cells (B), CFP-tagged ts-O45-G (C) and ts-O45-G at the plasma membrane (D) were acquired automatically with the high-content screening microscope. The images containing the Hoechst-stained cell nuclei were thresholded and subsequently binarised (pixels above the threshold value were set to 1, those below the threshold were set to 0) to define a digital mask of objects corresponding to the area occupied by each nucleus (dark grey areas in E). Manual inspections showed that on average 96 ± 4% of the cell nuclei were detected in this way. Cell nuclei touching each other or the border of the image were skipped from further analyses. The objects in this nuclear mask were then dilated (brighter ring-like grey areas in E) and the mask corresponding to the cell nuclei only was then subtracted to define a new digital mask with ring-like structures corresponding to juxtanuclear cytoplasmic parts of the cell. This new mask was then multiplied with image C and resulted in image F. A mask encompassing the nuclear and juxtanuclear ring-like structures together (dark and bright areas together in E) was then multiplied with the images D (ts-O45-G at the plasma membrane) and B (transfected YFP) resulting in images G and H, respectively. Finally, the fluorescence in images F to H was quantified for each object. Transport of ts-O45-G to the plasma membrane was then determined for each cell as the ratio (named 'Pm/tot.') of the fluorescences measured for corresponding objects in images G (ts-O45-G at the plasma membrane) and F (related to the total cellular amount of YFP-tagged ts-O45-G).

Golgi morphology in cells transfected with CFP- or YFP-tagged proteins, were developed. An example of the secretion assay is shown in Fig. 1. As transport marker, the temperature sensitive transmembrane protein ts-O45-G fused to CFP or YFP is used. It accumulates in the ER at 39.5°C and is transported to the plasma membrane at 32°C where it can be detected by a monoclonal antibody recognising an extracellular epitope of ts-O45-G (see [10]). The ratio of ts-O45-G spe-

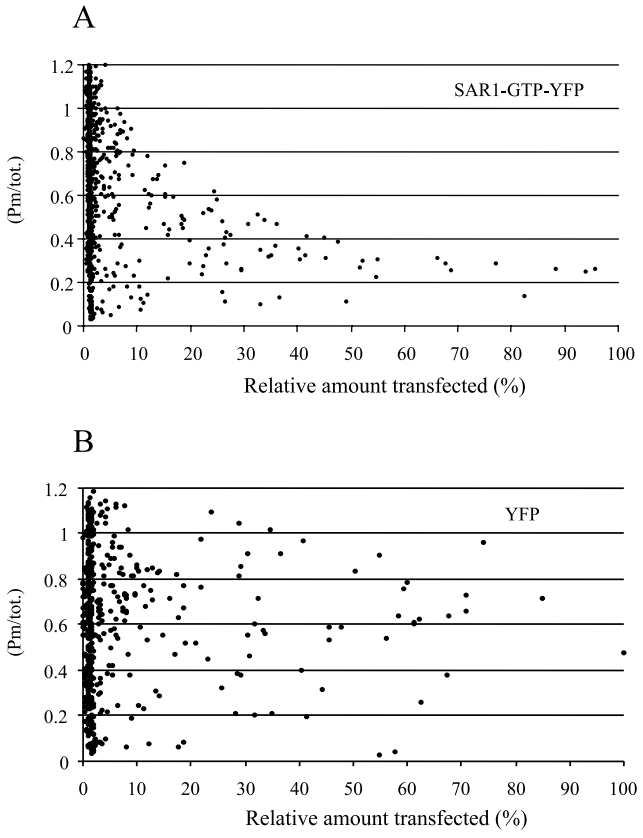

Fig. 2. Detection of transport inhibition with the secretion assay. Transport of ts-O45-G was analysed with the high-content screening microscope in samples transfected with plasmid encoding SAR1-GTP-YFP (A) or YFP (B) as a control. Transport of ts-O45-G (Pm/tot. see legend to Fig. 1 for its definition) and the amount of GFP proteins expressed in each individual cell was quantified as described in the legend to Fig. 1 and in the text. Shown are scatter plots relating the relative amounts of ts-O45-G transported to the plasma membrane (Pm/tot.) versus the amounts of GFP proteins expressed. The latter ones were normalised and the minimum and maximum values obtained were set to 0 and 100%, respectively. The cells expressing less than 5% or more than 20% of the maximum were scored as non-transfected or overexpressing cells, respectively. The average transport of ts-O45-G was 0.65 ± 0.02 in non-transfected cells and 0.61 ± 0.04 or 0.36 ± 0.02 in YFP or YFP-SAR1-GTP overexpressing cells, respectively.

cific plasma membrane fluorescence (antibody staining) and total CFP- or YFP-ts-O45-G fluorescence determines the relative amount of ts-O45-G transported (abbreviated in the following 'Pm/tot.'). In order to test this assay, a YFP-tagged SAR1 mutant (H79G, named SAR1-GTP-YFP in the following), which only slowly hydrolyses GTP and is known to inhibit transport away from the ER [11], was transfected and ts-O45-G transport measured as a function of the amount of expressed SAR1-GTP-YFP. As shown in Fig. 2 ts-O45-G transport to the plasma membrane decreased with increasing amounts of transfected SAR1-GTP-YFP. In cells transfected with YFP alone no such inhibition was detected. In two independent experiments with more than 700 cells analysed Pm/tot. was determined to 0.65 ± 0.02, 0.61 ± 0.04 and 0.36 ± 0.02 for non-transfected, YFP and SAR1-GTP-YFP overexpressing cells, respectively (see legend to Fig. 2 for definitions). This demonstrates that the automated assay developed is capable of identifying transport inhibitors such as the SAR1-GTP-YFP when expressed in cells.

An important feature of a microscope-based screening system is that it should offer quantitative information on the spatial distribution of the signals of interest in single cells. In order to test the performance of our screening system in this context we developed and tested a further assay, which probes the morphology of the Golgi complex (Fig. 3). This organelle is central to the secretory pathway and its proper functioning is of vital importance for transport and processing of secretory cargo. Golgi morphology changes when the flow of membrane transport towards or away from it is altered and is thus often an indication of imbalanced membrane flow through the secretory pathway. For example, treatment of cells with the microtubule depolymerising drug nocodazole inhibits transport of membrane-bounded cargo carriers [12] and the Golgi becomes scattered throughout the entire cell cytoplasm into numerous Golgi ministacks (see Fig. 3 and [13]). The Golgi integrity assay described here was developed to detect such phenotype and thus scores the number, intensity and size of Golgi fragments. In order to test it, cells were treated with 10 μM nocodazole for 8 h and Golgi morphology was analysed in comparison to non-treated control cells (see Fig. 3). Consistent with visual inspections the number of Golgi fragments detected by the screening microscope system increased from 3.8 ± 0.7 to 50 ± 7.0 in control and nocodazole-treated cells, respectively. In parallel, the average size and intensities of Golgi ministacks in nocodazole-treated cells were determined to decrease to $12 \pm 4\%$ and $74 \pm 3\%$ of the values obtained for control cells. Such decrease in intensity and size of Golgi fragments is consistent with the hypothesis that during nocodazole treatment the total amount of the Golgi marker used does not change drastically in contrast to the Golgi morphology. Altogether, this demonstrates that the Golgi integrity assay described here is able to detect phenotypes that resemble Golgi fragmentation in response to nocodazole.

We presently apply the system and assays described here to systematic analyses in cells overexpressing GFP-tagged proteins of unknown function as they are identified by large-scale gene sequencing projects such as that of the German cDNA Consortium [14]. This has demonstrated so far that hundreds of proteins can be analysed in parallel with our system and more than 30 proteins which inhibit protein secretion or affect the morphology of the Golgi complex upon overexpression have already been identified (Starkuviene et al., unpublished results).

In conclusion, the modular microscope-based screening platform described here has applications in large-scale functional analysis of proteins of unknown function. It automatically acquires high-quality multicolour image data, which enables quantitative screens based on cell or organelle morphology as exemplified here by the Golgi integrity assay. An important feature of the system is that it also includes automated collection of bioinformatic data, which is essential for systematic analyses of the functional interrelationship of the proteins of interest in larger networks. The system can be easily adapted to implement new developments due to its modular nature and means of data organisation. Therefore, only few changes on the system will be necessary for applications different from the ones shown here such as in drug screening or for the systematic functional analysis of proteins by gene-knockdowns using siRNAs.

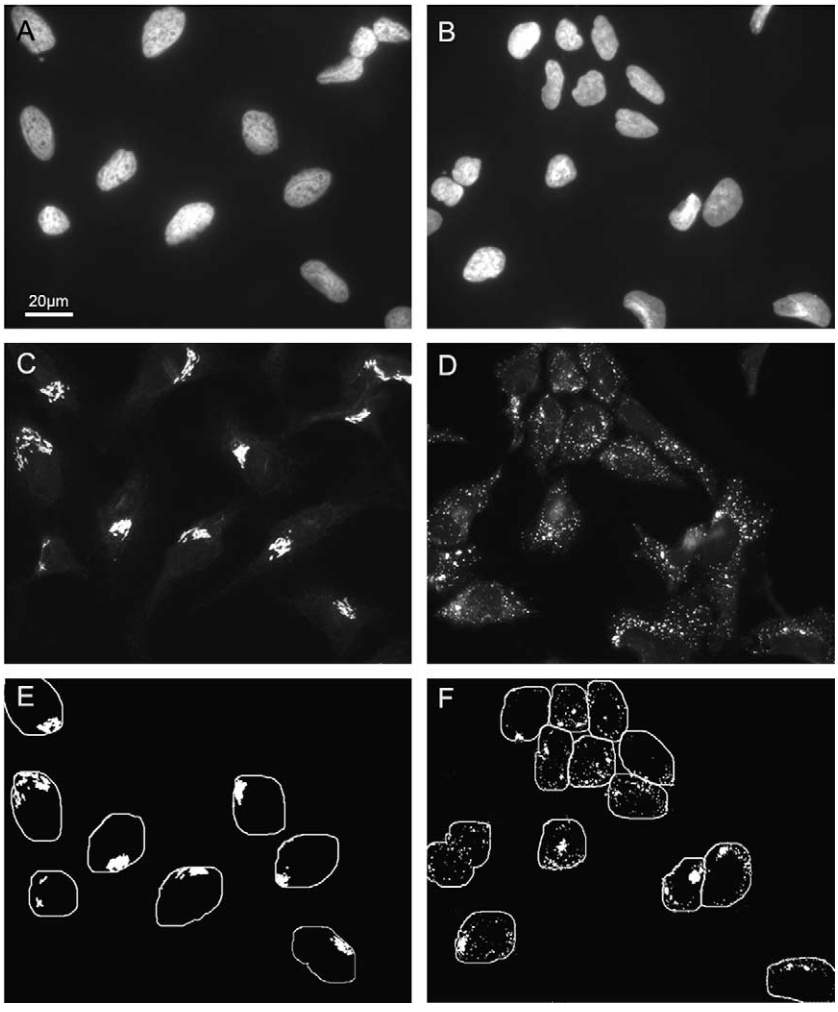

Fig. 3. Example of the Golgi integrity assay. HeLa cells, non-treated (A,C,E) or treated (B,D,F) with 10 μM nocodazole for 8 h, were stained with Hoechst dye (A,B) and a monoclonal antibody recognising the Golgi matrix protein GM130 [15] (C,D). Nuclear and cytoplasmic juxtanuclear regions were determined as described in the legend to Fig. 1. The images containing Golgi labelling were further thresholded and binarised (E,F) and the number, intensity and size of thresholded Golgi fragments present in the nuclear and juxtanuclear area (rings around the cells in E and F) were determined.

Acknowledgements: We thank Kai Simons for antibodies and Brigitte Joggerst for technical assistance. This work has been supported by the BMBF with grant 01GR0101 of the National Genome Research Network (NGFN); and with grants 01KW9987 (German cDNA Consortium), 01KW0012 (DKFZ) and 01KW0013 (EMBL) within the German Genome Project (DHGP).

References

[1] Sawin, K.E. and Nurse, P. (1996) Proc. Natl. Acad. Sci. USA 93, 15146–15151.
[2] Gonzalez, C. and Bejarano, L.A. (2000) Trends Cell Biol. 10, 162–165.
[3] Simpson, J.C., Wellenreuther, R., Poustka, A., Pepperkok, R. and Wiemann, S. (2000) EMBO Rep. 1, 287–292.
[4] Ding, D.Q., Tomita, Y., Yamamoto, A., Chikashige, Y., Haraguchi, T. and Hiraoka, Y. (2000) Genes Cells 5, 169–190.
[5] Bastiaens, P.I. and Pepperkok, R. (2000) Trends Biochem. Sci. 25, 631–637.
[6] Wouters, F.S., Verveer, P.J. and Bastiaens, P.I. (2001) Trends Cell Biol. 11, 203–211.
[7] Ghosh, R.N., Chen, Y.T., DeBiasio, R., DeBiasio, R.L., Conway, B.R., Minor, L.K. and Demarest, K.T. (2000) Biotechniques 29, 170–175.
[8] Jessen, T. (2000) Drug Discov. Today 5, 49.
[9] Keller, P., Toomre, D., Diaz, E., White, J. and Simons, K. (2001) Nat. Cell Biol. 3, 140–149.
[10] Pepperkok, R., Lowe, M., Burke, B. and Kreis, T.E. (1998) J. Cell Sci. 111, 1877–1888.
[11] Aridor, M., Fish, K.N., Bannykh, S., Weissman, J., Roberts, T.H., Lippincott-Schwartz, J. and Balch, W.E. (2001) J. Cell Biol. 152, 213–229.
[12] Presley, J.F., Cole, N.B., Schroer, T.A., Hirschberg, K., Zaal, K.J. and Lippincott-Schwartz, J. (1997) Nature 389, 81–85.
[13] Cole, N.B., Sciaky, N., Marotta, A., Song, J. and Lippincott-Schwartz, J. (1996) Mol. Biol. Cell 7, 631–650.
[14] Wiemann, S., Weil, B., Wellenreuther, R., Gassenhuber, J. and Glassl, S. et al. (2001) Genome Res. 11, 422–435.
[15] Nakamura, N., Rabouille, C., Watson, R., Nilsson, T., Hui, N., Slusarewicz, P., Kreis, T.E. and Warren, G. (1995) J. Cell Biol. 131, 1715–1726.